Automatica 107 (2019) 61–67

Contents lists available at ScienceDirect

Automatica

journal homepage: www.elsevier.com/locate/automatica

Brief paper

Algebraic topological characterizations of structural balance in signed graphs☆

Baike She [a], Zhen Kan [b,*]

[a] Department of Mechanical Engineering, The University of Iowa, Iowa City, IA, 52246, USA
[b] Department of Automation, University of Science and Technology of China, Hefei, Anhui, 230052, China

ARTICLE INFO

Article history:
Received 29 May 2018
Received in revised form 18 March 2019
Accepted 4 May 2019
Available online xxxx

ABSTRACT

Algebraic topological characterizations of the structural balance in signed graphs are considered in this work. Leveraging tools from the algebraic topology, simplicial complexes are used instead of conventional graphical approaches to model signed graphs and capture their global topological properties. Topological invariants, such as homology and cohomology, are then explored to extract topological characterizations of the structural balance from the simplicial-complex-based models. The developed topological characterizations reveal that the structural balance is closely related to the first homology and cohomology of the modeled simplicial complex. Examples are provided to demonstrate the developed topological insights of the structural balance and how it can be leveraged to construct networks with desired topologies.

1. Introduction

Dynamic networks exist widely in natural, social, and engineering systems, such as neural networks (Crossley, Mechelli, Vértes, Winton-Brown, Patel, Ginestet, McGuire, and Bullmore, 2013), social networks (Girvan & Newman, 2002), networked robotic systems (Olfati-Saber, Fax, & Murray, 2004), power networks (Fang, Misra, Xue, & Yang, 2012), and sensor networks (Choi & How, 2011). To study such dynamic networks, unsigned graphs that only admit positive edge weights have long been a research focus in modeling collaborative networks. Average consensus (Ren, Beard, & Atkins, 2007), formation control (Kan, Dani, Shea, & Dixon, 2012), and flocking (Tanner, Jadbabaie, & Pappas, 2007) are typical applications, where agents positively evaluate information collected from neighboring agents and coordinate to perform network-wide goals. A key assumption in most of the aforementioned results is that the dynamic network is inherently collaborative. However, practical networks are not necessarily collaborative and can even be competitive. For instance, agents may compete for the use of bandwidth in a communication network (Yaïche, Mazumdar, & Rosenberg, 2000), and individuals tend to have friend/adversary or trust/distrust relationships in social networks (Jackson, 2010). Therefore, signed graphs that allow positive and negative edge weights are more plausible in modeling practical networks with collaborative and competitive interactions.

The structural balance is a topological characterization of signed graphs (Harary et al., 1953). Roughly speaking, the structural balance indicates the capability of dividing a network into two subgroups such that nodes within each subgroup have only collaborative relationships (i.e., positive edges), while nodes from different subgroups are connected by antagonistic relationships (i.e., negative edges). Recent research shows that the structural balance is crucial in determining the network performance. For instance, the bipartite consensus over a network with antagonistic interactions was established in Altafini (2013) provided that the network is structurally balanced. The developed bipartite consensus was then extended for signed directed networks (Jiang, Zhang, & Chen, 2017), signed switching networks (Meng, Meng, & Hong, 2018), general linear agents (Zhang & Chen, 2017), and high-order system dynamics (Wu, Zhao, & Hu, 2017). Despite various system dynamics and network topologies, the structural balance is a common necessary condition for achieving bipartite consensus in the aforementioned results (Altafini, 2013; Jiang et al., 2017; Meng et al., 2018; Wu et al., 2017; Zhang & Chen, 2017). Besides engineering applications, the structural balance has also been explored in the context of social and opinion networks (Antal, Krapivsky, & Redner, 2005; Kunegis, 2014; Marvel, Kleinberg, Kleinberg, & Strogatz, 2011; Proskurnikov, Matveev, & Cao, 2016) to reveal the evolution of individual's social states in the presence of trustful and distrustful interactions. Recent research also indicates that the structural balance

☆ The material in this paper was not presented at any conference. This paper was recommended for publication in revised form by Associate Editor Florian Dorfler under the direction of Editor Christos G. Cassandras.

* Corresponding author.
E-mail addresses: baike-she@uiowa.edu (B. She), zkan@ustc.edu.cn (Z. Kan).

https://doi.org/10.1016/j.automatica.2019.05.029

provides insights in addressing network stabilization and controllability (Alemzadeh, de Badyn, & Mesbahi, 2017; de Badyn, Alemzadeh, & Mesbahi, 2017; Liu, Chen, & Başar, 2016; Sun, Hu, & Xie, 2017). The verification and prediction of the structural balance in signed networks were investigated from a data-driven perspective in Pan, Shao, and Mesbahi (2016).

Due to the significance of the structural balance in network performance, this work is particularly motivated to investigate the fundamental relationship between the structural balance and the underlying topological structure of signed graphs. Different from existing graph theoretic approaches, algebraic topology is explored. Drawing on techniques from algebraic topology, algebraic topological spaces and invariants are exploited to extract the topological properties of the structural balance in signed graphs. Specifically, instead of using conventional graphs, simplicial complexes are employed as the primary tool to model the signed graph. As a generalization of conventional graphical models, simplicial complexes are able to capture the global topological properties of the signed graph. Topological invariants, such as homology and cohomology, are then explored to extract topological characterizations of the structural balance from the simplicial-complex-based models. The developed topological characterizations reveal the fundamental relationship between the structural balance and the underlying network topology by showing that the structural balance is closely related to the first homology and cohomology of the modeled simplicial complex. In particular, the vanishing first homology and cohomology along with positive 3-node circular subgraphs are found to be sufficient to lead to a structurally balanced network. Examples are provided to demonstrate the developed topological insights of the structural balance and how it can be leveraged to construct networks with desired topologies.

The contributions of this work are multi-fold. First, simplicial complexes are used as a novel modeling approach to represent and analyze signed networks. Compared to conventional graphical models, simplicial complexes generalize graphical models in the sense that, in addition to the binary relations between nodes as in standard graphs, they also capture the higher-order topological relations among them (Hatcher, 2001). Consequently, simplicial complexes are able to provide insights into network topologies that are unobtainable from standard graphs or other traditional modeling and analysis methods. Second, the use of the simplicial complex opens a new door to investigate networks, where new sets of analysis tools from algebraic topology become available. In particular, as topological invariants that can only be extracted from simplicial complexes, homology and cohomology are exploited to unravel the fundamental relationship between the structural balance and the network topology. Motivated by the recent research of using homology to verify sensor network coverage (Chintakunta & Krim, 2014; De Silva & Ghrist, 2006; Tahbaz-Salehi & Jadbabaie, 2010), the homology and cohomology are extended in this work to unravel the topological properties of signed graphs, which has received little research attention in the literature.

2. Problem formulation

Consider a multi-agent system with cooperative and antagonistic interactions represented by an undirected signed graph $\mathcal{G} = (\mathcal{V}, \mathcal{E}, \mathcal{W})$, where the node set $\mathcal{V} = \{v_1, \ldots, v_n\}$ and the edge set $\mathcal{E} \subset \mathcal{V} \times \mathcal{V}$ represent the agents and the interactions between pairs of agents, respectively. Let $w_{ij}: \mathcal{E} \to \{\pm 1\}$ denote the weight associated with the edge $\left(v_i, v_j\right) \in \mathcal{E}$. If $w_{ij} = 1$, v_i and v_j are called positive neighbors and negative neighbors if $w_{ij} = -1$. Positive neighborhood indicates cooperative interactions while negative neighborhood indicates competitive interactions. The interactions within $\mathcal{G}$ are then captured by the adjacency matrix $\mathcal{W} = \left[w_{ij}\right] \in \mathbb{R}^{n\times n}$, where $w_{ij} = 0$ if $\left(v_i, v_j\right) \notin \mathcal{E}$. No self-loop is considered, i.e., $w_{ii} = 0\ \forall i = 1, \ldots, n$. A path of length k in $\mathcal{G}$ is a concatenation of distinct edges $\{(v_1, v_2), (v_2, v_3), \ldots, (v_k, v_{k+1})\} \subset \mathcal{E}$. A circular subgraph[1] of length k in $\mathcal{G}$ is a path with identical starting and end node, i.e., $v_1 = v_{k+1}$. Graph $\mathcal{G}$ is connected if there exists a path between any pair of nodes in $\mathcal{V}$.

Definition 1 (*Altafini, 2013*). A connected signed graph $\mathcal{G} = (\mathcal{V}, \mathcal{E}, \mathcal{W})$ is structurally balanced if the node set $\mathcal{V}$ can be partitioned into $\mathcal{V}_1$ and $\mathcal{V}_2$ with $\mathcal{V}_1 \cup \mathcal{V}_2 = \mathcal{V}$ and $\mathcal{V}_1 \cap \mathcal{V}_2 = \emptyset$, where $w_{ij} > 0$ if $v_i, v_j \in \mathcal{V}_q$, $q \in \{1, 2\}$, and $w_{ij} < 0$ if $v_i \in \mathcal{V}_q$ and $v_j \in \mathcal{V}_r$, $q \neq r$, and $q, r \in \{1, 2\}$. Otherwise it is structurally unbalanced.

Definition 1 indicates that, for a structurally balanced graph, the nodes within the same subgroup (i.e., $\mathcal{V}_1$ or $\mathcal{V}_2$) contain only positive neighbors, while nodes from different subgroups are negative neighbors. Based on Definition 1, various graph theoretic characterizations of the structural balance were developed in the literature (Altafini, 2013; Aref & Wilson, 2017; Harary, 1960; Harary & Kabell, 1980). As a complement to the existing results, rather than using traditional graph theoretic approaches as in Altafini (2013), Aref and Wilson (2017), Harary (1960) and Harary and Kabell (1980), the objective of this work is to characterize the structural balance of signed graphs based on a new perspective from algebraic topology, and exploits algebraic topological tools to develop topological insights of the structural balance.

3. Algebraic topological characterizations of structural balance

Topological characterizations of the structural balance in signed graphs are developed in this section. To facilitate the development, algebraic topology is briefly reviewed in Section 3.1 (cf. Hatcher, 2001, for a detailed explanation). Leveraging tools from algebraic topology, topological characterizations of the structural balance are extracted in Section 3.2. Examples are provided in Section 3.3 to elaborate on the developed topological characterizations.

3.1. Background on simplicial complex, homology, and cohomology

Let $\mathcal{V} = \{v_i\}$, $i \in \{0, \ldots, n-1\}$, be a finite set of n points. A k-*simplex* σ_k (or a k-dimensional simplex) is a k-dimensional convex polyhedron formed by an unordered set $\{v_0, \ldots, v_k\} \subseteq \mathcal{V}$ with $v_i \neq v_j$ for all $i \neq j$. The faces of the σ_k consist of $(k-1)$-simplices of the form $\{v_0, \ldots, v_{i-1}, v_{i+1}, \ldots, v_k\}$ for $0 \leq i \leq k$. A*simplicial complex X* is then defined as a finite collection of simplices closed with respect to the inclusion of faces. In terms of geometrical realization, a simplicial complex is a combinatorial object composed of simplices, where graphical components (e.g., nodes, edges, and cliques[2]) can be represented by simplices of various dimensions. In addition to binary relations by edges in conventional graphs, a simplicial complex also captures higher-order relations among a set of nodes by simplices of higher dimensions. Simplicial complexes thereby represent a generalization of traditional graphs, providing a global topological characterization of graphs.

[1] Circular subgraphs, instead of cycles, are used to avoid potential confusions with the topological definition of k-cycles in the simplicial-complex-based models.

[2] A clique is a complete graph formed by a subset of nodes.

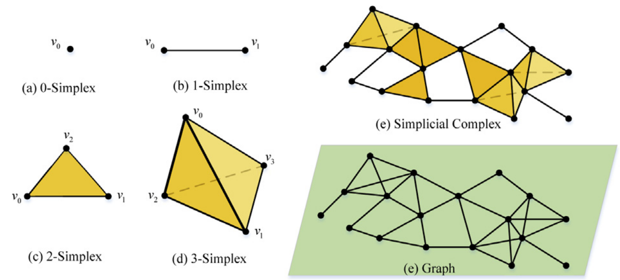

Fig. 1. The illustration of the simplices and the simplicial complex.

Example 1. To illustrate the simplicial complex, graphical examples are provided in Fig. 1. Fig. 1(a) and (b) show that nodes and edges in graphs are 0-simplices and 1-simplices, respectively. Fully connected subsets of nodes (i.e., cliques) can be represented by higher-order simplices. For instance, a complete graph of 3 nodes corresponds to a 2-simplex (i.e., a triangle) in Fig. 1(c), while a complete graph of 4 nodes corresponds to a 3-simplex (i.e., a tetrahedron) in Fig. 1(d). Fig. 1(e) shows the construction of a simplicial complex from a conventional graph, where the graph at the bottom can be considered as the projection of the simplicial complex onto a 2D plane, in which all simplices with dimension greater than 1 are neglected. Note that, in Fig. 1(e), the edge connections in the graph at the bottom are preserved in the simplicial complex by the 0-simplices and 1-simplices. No existing relationships are lost when modeling a graph by a simplicial complex. Therefore, any features that can be extracted from graphs are preserved in the corresponding simplicial complex.

An orientation of a k-simplex is induced by an ordering of its vertices, where two orderings are equivalent if and only if one can be obtained from the other by an even permutation. In particular, A *k-simplex* $\{v_0, \ldots, v_k\}$ with an ordering is denoted by $[v_0, \ldots, v_k]$, and a change in the ordering corresponds to a change in the sign of the simplex, i.e., $\left[v_0, \ldots, v_i, \ldots, v_j, \ldots, v_k\right] = -\left[v_0, \ldots, v_j, \ldots, v_i, \ldots, v_k\right]$. Given an oriented simplicial complex[3] X, for each $k \geq 0$, $C_k(X; \mathbb{Z})$ is a free abelian group whose basis is the set of oriented k-simplices $\sigma_k \in X$. The elements of $C_k(X; \mathbb{Z})$ are called *k-chains*, where a k-chain is defined as a sum of the form $\sum_j a_j \sigma_j^{(k)}$ with $a_j \in \mathbb{Z}$ and $\sigma_j^{(k)}$ denoting an oriented k-simplex σ_k. From the definition of k-chains, the vector space $C_k(X; \mathbb{Z})$ is clearly an additive abelian group.[4] It is worth pointing out that other types of abelian groups, such as multiplicative abelian groups, are also applicable. The dimension of X is the maximum dimension of its simplices. If k is larger than the dimension of X, $C_k(X; \mathbb{Z}) = 0$.

[3] Oriented simplicial complexes are used throughout in this work. Please note that oriented simplicial complexes are different from ordered simplicial complexes which are simply simplicial complexes with ordered vertices. For instance, $[a, b, c]$ and $[c, a, b]$ are two different ordered 2-simplexes as the vertices have different orders, while $[a, b, c]$ and $[c, a, b]$ are the same orientated 2-simplexes as $[c, a, b] = -[a, c, b] = [a, b, c]$.

[4] An additive abelian group $(G, +)$ is a set G together with a binary operation $+: G \times G \to G$ satisfying the following axioms: (1) associativity: $(a + b) + c = a + (b + c)$ for all $a, b, c \in G$; (2) commutativity: $a + b = b + a$ for all $a, b \in G$; (3) identity element is 0 satisfying $a + 0 = a$ for each $a \in G$; and (4) the inverse element $a^{-1} = -a$ for each $a \in G$ such that $a + (-a) = 0$ (Durbin, 2008). Some examples of additive abelian groups are the set of integers $\mathbb{Z}$, the set of rationals $\mathbb{Q}$, and the set of reals $\mathbb{R}$.

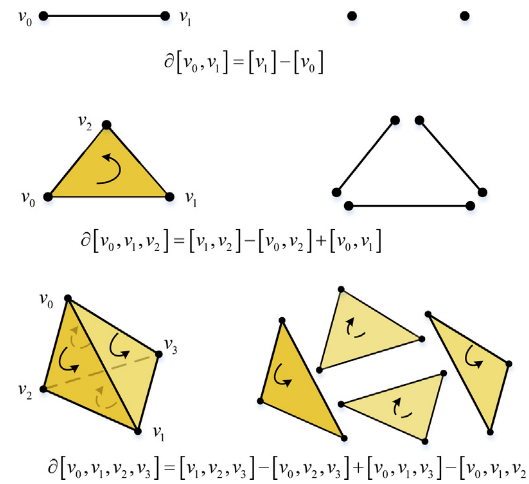

Fig. 2. The boundary maps of an oriented 1-simplex, 2-simplex, and 3-simplex.

The kth simplicial boundary map is a homomorphism[5] $\partial_k: C_k(X; \mathbb{Z}) \to C_{k-1}(X; \mathbb{Z})$ defined as

$$\partial_k [v_0, \ldots, v_k] = \sum_{j=0}^{k} (-1)^j \left[v_0, \ldots, \hat{v}_j, \ldots, v_k\right], \tag{1}$$

where $\hat{v}_j$ indicates that v_j is removed from the sequence $v_0, \ldots, v_k$. A *chain complex* is a sequence of homomorphism,

$$\cdots \xrightarrow{\partial_{k+2}} C_{k+1} \xrightarrow{\partial_{k+1}} C_k \xrightarrow{\partial_k} C_{k-1} \xrightarrow{\partial_{k-1}} \cdots, \tag{2}$$

where the homomorphism ∂_k satisfies $\partial_{k-1} \circ \partial_k = 0$ (Hatcher, 2001), i.e., the image of ∂_k is included in the kernel of ∂_{k-1}.

Example 2. Fig. 2 illustrates the boundary maps on oriented simplices. For instance, the oriented 1-simplex $[v_0, v_1]$ corresponds to an edge, where the boundary map in (1) yields $\partial_1 [v_0, v_1] = [v_1] - [v_0]$. Similarly, a 2-simplex $[v_0, v_1, v_2]$ corresponds to a triangle with the boundary map $\partial_2 [v_0, v_1, v_2] = [v_1, v_2] - [v_0, v_2] + [v_0, v_1]$, while a 3-simplex $[v_0, v_1, v_2, v_3]$ corresponds to a tetrahedron with the boundary map $\partial_3 [v_0, v_1, v_2, v_3] = [v_1, v_2, v_3] - [v_0, v_2, v_3] + [v_0, v_1, v_3] - [v_0, v_1, v_2]$.

As basic building blocks for simplicial homology, the *k-cycles* and the *k-boundaries* are defined as

$$\begin{aligned} k\text{-cycles: } \ker \partial_k &= \{x \in C_k |\, \partial_k x = 0\}, \\ k\text{-boundaries: } \operatorname{img} \partial_{k+1} &= \{x \in C_k |\, \exists y \text{ s.t. } x = \partial_{k+1} y\}. \end{aligned} \tag{3}$$

Intuitively, $\ker \partial_k$ indicates a set of k-chains without boundary and therefore represent k-dimensional cycles in the simplicial complex X. Since some of the k-cycles also bound a subcomplex of dimension $k + 1$ in X, the k-boundaries in (3) particularly indicate a set of k-chains forming boundaries of higher-dimensional chains. Based on the k-cycles and the k-boundaries, the kth simplicial homology is defined as the quotient vector space

$$\mathcal{H}_k(X; \mathbb{Z}) \triangleq \ker \partial_k / \operatorname{img} \partial_{k+1}. \tag{4}$$

Consequently, $\mathcal{H}_k$ indicates the k-dimensional cycles that are not the boundaries of higher-dimensional chains, and the dimension of $\mathcal{H}_k$ is the number of "k-dimensional holes" in X.

[5] If $(A, \cdot)$ and $(B, *)$ are two abelian groups with operations $\cdot$ and $*$, a homomorphism is a mapping $f: A \to B$ satisfying $f(a \cdot b) = f(a) * f(b)$ for all $a, b \in A$ (Durbin, 2008).

For instance, the uncolored quadrilaterals of the simplicial complex in Fig. 1(e) are elements of the first homology group $\mathcal{H}_1$ indicating 1-dimensional holes, since the edges of the quadrilaterals form 1-cycles that are not the boundaries of any higher-dimensional simplices. Despite various types, the graphs can be topologically identical in terms of the number of k-dimensional cycles. As a topological invariant, $\mathcal{H}_k$ provides a characterization of topological structures of graphs.

Cohomology groups are constructed by turning chain groups C_k into groups of homomorphisms and boundary operators ∂_k into their dual homomorphisms. Specifically, given a chain group C_k and an abelian group $\mathcal{A}$, a *k-dimensional cochain* $C^k(X;\mathcal{A})$ is defined as a homomorphism $\varphi: C_k \to \mathcal{A}$, which maps elements in C_k to $\mathcal{A}$. Note that the cochains C^k are also abelian groups. A *cochain complex* is a dual notion to the chain complex in (2) as

$$\cdots \xrightarrow{\delta^{k-1}} C^{k-1} \xrightarrow{\delta^{k}} C^{k} \xrightarrow{\delta^{k+1}} C^{k+1} \xrightarrow{\delta^{k+2}} \cdots \tag{5}$$

where $\delta^k: C^{k-1} \to C^k$ represents the dual homomorphism to ∂_k, satisfying $\delta^{k+1}\circ\delta^k = 0$. The cochain complex in (5) represents maps between abelian groups C^k but with reversed arrows. The *k-cocycles* and the *k-coboundaries* are defined as

$$\begin{aligned} k\text{-cocycles: } \ker\delta^{k+1} &= \left\{x\in C^k \middle| \delta^{k+1}x = 0\right\},\\ k\text{-coboundaries: } \operatorname{img}\delta^{k} &= \left\{x\in C^k \middle| \exists y \text{ s.t. } x = \delta_k y\right\}. \end{aligned} \tag{6}$$

Based on k-cocycles and k-coboundaries, the kth cohomology is then defined as

$$\mathcal{H}^k(X;\mathcal{A}) \triangleq \ker\delta^{k+1}/\operatorname{img}\delta^k. \tag{7}$$

3.2. Homology and cohomology based characterizations of structural balance

To develop homology and cohomology based characterizations, we start from modeling the signed graph $\mathcal{G}$ by a simplicial complex $X_{\mathcal{G}}$, where existing methods in De Silva and Ghrist (2006), Hatcher (2001) and Tahbaz-Salehi and Jadbabaie (2010) can be used to construct $X_{\mathcal{G}}$. Based on the constructed $X_{\mathcal{G}}$, the cohomology-based topological characterization is developed first, followed by an extension to homology-based characterizations. Consider the group $\mathcal{A}$ in (7) taking the form of a multiplicative abelian group[6] $(\mathbb{Z}_2,\times)$ with the basis $\mathbb{Z}_2 = \{-1,1\}$ and the multiplication operation "$\times$". The multiplicative abelian group $(\mathbb{Z}_2,\times)$ is particularly motivated by the use of the product of edge weights. Let $\varphi: X_{\mathcal{G}} \to \mathbb{Z}_2$ be a group homomorphism mapping simplices in $X_{\mathcal{G}}$ to an element in $\mathbb{Z}_2$, i.e., each simplex is marked as -1 or $+1$. In particular, the homomorphism φ maps each edge (v_i,v_j) in $\mathcal{G}$ to its weight w_{ij}, i.e., $\varphi([v_i,v_j]) = w_{ij}$ where $[v_i,v_j]$ is the corresponding 1-simplex in $X_{\mathcal{G}}$. The cochain group $C^k(X_{\mathcal{G}};\mathbb{Z}_2)$ is thereby formed by $\varphi(\sigma_k)$, where σ_k denotes oriented k-simplices in $X_{\mathcal{G}}$.

The cochain complex on $X_{\mathcal{G}}$ with the group $(\mathbb{Z}_2,\times)$ is defined as

$$\cdots \xrightarrow{\delta^{k-1}} C^{k-1}(X_{\mathcal{G}};\mathbb{Z}_2) \xrightarrow{\delta^{k}} C^{k}(X_{\mathcal{G}};\mathbb{Z}_2) \xrightarrow{\delta^{k+1}} \cdots, \tag{8}$$

where the coboundary δ^k maps an element in $C^{k-1}(X_{\mathcal{G}};\mathbb{Z}_2)$ to an element in the group $C^k(X_{\mathcal{G}};\mathbb{Z}_2)$. Specifically, given an oriented $(k-1)$-simplex $[v_0,\ldots,v_{k-1}]$ and an oriented k-simplex $[v_0,\ldots,v_k]$,

$$\begin{aligned} \delta^k\varphi([v_0,\ldots,v_{k-1}]) &= \varphi([v_0,\ldots,v_k]) \\ &= \prod_{j=0}^{k}\varphi^{(-1)^j}\left([v_0,\ldots,\hat{v}_j,\ldots,v_k]\right) \end{aligned} \tag{9}$$

where $\hat{v}_j$ indicates that v_j is removed and φ^{-1} denotes the inverse element in $(\mathbb{Z}_2,\times)$. Due to the consideration of a multiplicative abelian group, $\varphi([v_0,\ldots,v_k])$ in (9) is written as products, rather than the sums in (1) as an additive abelian group. For instance, given a 0-simplex v_0 and a 1-simplex $[v_0,v_1]$ in $X_{\mathcal{G}}$, the coboundary δ^1 mapping $\varphi(v_0)\in C^0(X_{\mathcal{G}};\mathbb{Z}_2)$ to $\varphi([v_0,v_1])\in C^1(X_{\mathcal{G}};\mathbb{Z}_2)$ by $\delta^1\varphi(v_0) = \varphi([v_0,v_1]) = \varphi(v_1)\varphi^{-1}(v_0) = \varphi(v_0)\varphi(v_1)$, where the fact that $\varphi^{-1}(v_0)\varphi(v_0) = 1$ in $(\mathbb{Z}_2,\times)$ is used.

Based on the cochain complex in (8), the kernel group $\ker\delta^{k+1}$ is defined as

$$\ker\delta^{k+1} = \{x\in C^k(X_{\mathcal{G}};\mathbb{Z}_2) \mid \delta^{k+1}x = 1\}, \tag{10}$$

where $\delta^{k+1}x = 1$ indicates that 1 is the identity element of the multiplicative abelian group. Similar to (6) and (7), the $\operatorname{img}\delta^k$ of $C^k(X_{\mathcal{G}};\mathbb{Z}_2)$ and the kth cohomology are defined as

$$\operatorname{img}\delta^k = \left\{x\in C^k(X_{\mathcal{G}};\mathbb{Z}_2) \middle| \exists y \text{ s.t. } x = \delta^k y\right\}, \tag{11}$$

and

$$\mathcal{H}^k(X_{\mathcal{G}};\mathbb{Z}_2) \triangleq \ker\delta^{k+1}/\operatorname{img}\delta^k, \tag{12}$$

respectively.

Lemma 1. *Consider a signed graph $\mathcal{G}$ modeled by a simplicial complex $X_{\mathcal{G}}$. Suppose that there exists a circular subgraph in $\mathcal{G}$ composed of three vertices $\{v_i,v_j,v_k\}$, which corresponds to an oriented 2-simplex $[v_i,v_j,v_k]$ in $X_{\mathcal{G}}$. The circular subgraph is positive if and only if $\varphi([v_i,v_j])\in\ker\delta^2$.*

Proof. To prove the sufficient condition, if $\varphi([v_i,v_j])\in\ker\delta^2$, the definition of cocycles in (10) implies $\delta^2\varphi([v_i,v_j]) = 1$. Since $[v_i,v_j,v_k]$ is a 2-simplex containing $[v_i,v_j]$, the homomorphism yields

$$\begin{aligned} \delta^2\varphi([v_i,v_j]) &= \varphi([v_i,v_j,v_k]) \\ &= \varphi([v_j,v_k])\varphi^{-1}([v_i,v_k])\varphi([v_i,v_j]) \\ &= \varphi([v_j,v_k])\varphi([v_k,v_i])\varphi([v_i,v_j]) = 1, \end{aligned}$$

where $\varphi^{-1}([v_i,v_k]) = \varphi([v_k,v_i])$ is due to the change of the ordering of vertices. Since φ maps an edge in $\mathcal{G}$ to its edge weight, $\varphi([v_j,v_k])\varphi([v_k,v_i])\varphi([v_i,v_j]) = 1$ indicates that the product of the edge weights is one. Therefore, the circular subgraph composed of $\{v_i,v_j,v_k\}$ is a positive cycle.

To prove the necessary condition, if the circular subgraph with nodes $\{v_i,v_j,v_k\}$ in $\mathcal{G}$ is positive,

$$\begin{aligned} 1 &= \varphi([v_j,v_k])\varphi([v_k,v_i])\varphi([v_i,v_j]) \\ &= \varphi([v_j,v_k])\varphi^{-1}([v_i,v_k])\varphi([v_i,v_j]) \\ &= \delta^2\varphi([v_i,v_j]), \end{aligned}$$

which indicates that $\varphi([v_i,v_j])\in\ker\delta^2$. □

Theorem 1. *Given the simplicial complex $X_{\mathcal{G}}$ modeling the signed graph $\mathcal{G}$, $\mathcal{G}$ is structurally balanced if all 3-node circular subgraphs (i.e., circles composed of three vertices $\{v_i,v_j,v_k\}$) are positive and the first cohomology satisfies $\mathcal{H}^1(X_{\mathcal{G}};\mathbb{Z}_2) = 0$.*

Proof. According to (12), the first cohomology $\mathcal{H}^1(X_{\mathcal{G}};\mathbb{Z}_2)$ is defined as a quotient vector space of $\ker\delta^2$ and $\operatorname{img}\delta^1$. If $\mathcal{H}^1 = 0$,

[6] A multiplicative abelian group $(G,\times)$ is a set G together with a binary multiplication operation $\times$ that maps the product $c = ab$ to G for any $a,b\in G$. The multiplicative abelian group $(G,\times)$ is associative (i.e., $(ab)c = a(bc)$ for all $a,b,c\in G$) and commutative (i.e., $ab = ba$ for all $a,b\in G$). In addition, for each $a\in G$, there exists an identity element of 1 satisfying $a\times 1 = a$ and an inverse element of a^{-1} such that $aa^{-1} = 1$. For instance, the integers $\mathbb{Z}\setminus\{0\}$, the rationals $\mathbb{Q}\setminus\{0\}$, and the reals $\mathbb{R}\setminus\{0\}$ are all multiplicative abelian groups.

then

$$\ker \delta^2 = \operatorname{img} \delta^1, \tag{13}$$

which indicates that the set of 1-cocycles (i.e., $\ker \delta^2$) coincides with the set of 1-coboundaries (i.e., $\operatorname{img} \delta^1$). If all 3-node circular graphs $\{v_i, v_j, v_k\}$ in $\mathcal{G}$ are positive, by Lemma 1, we know that $\varphi([v_j, v_k])\varphi([v_k, v_i])\varphi([v_i, v_j]) = 1$ and $\varphi([v_i, v_j]) \in \ker \delta^2$. From (13), $\varphi([v_i, v_j])$ also belongs to $\operatorname{img} \delta^1$. Therefore, there exists a 0-simplex v_i that can be mapped to $[v_i, v_j]$ by the definition of k-coboundary in (11).

Due to the consideration of $(\mathbb{Z}_2, \times)$, the homomorphism $\varphi(v_i)$ also maps the 0-simplex v_i in $X_\mathcal{G}$ (i.e., the node v_i in $\mathcal{G}$) to either -1 or 1. Clearly, $C^0(X_\mathcal{G}; \mathbb{Z}_2)$ is an abelian group with $\varphi(v_i)$ as its basis. Suppose that the node set $\mathcal{V}$ in $\mathcal{G}$ can be partitioned into two sets $\mathcal{V}_1$ and $\mathcal{V}_2$, where $\mathcal{V}_1 \cap \mathcal{V}_2 = \emptyset$ and $\mathcal{V}_1 \cup \mathcal{V}_2 = \mathcal{V}$. Without loss of generality, let $\varphi(v_i) = 1$ if $v_i \in \mathcal{V}_1$ and $\varphi(v_i) = -1$ otherwise. If an edge (v_i, v_j) in $\mathcal{G}$ is positive, its corresponding 1-simplex $[v_i, v_j]$ in $X_\mathcal{G}$ satisfies

$$\varphi([v_i, v_j]) = \varphi(v_i)\varphi(v_j) = 1, \tag{14}$$

which can only be true when $\varphi(v_i)$ and $\varphi(v_j)$ are both positive or both negative. Therefore, $\varphi([v_i, v_j]) = 1$ in (14) indicates that v_i and v_j are from the same set, i.e., either both from $\mathcal{V}_1$ or both from $\mathcal{V}_2$. Analogously, if an edge (v_i, v_j) in $\mathcal{G}$ is negative, $\varphi([v_i, v_j]) = -1$ indicates that v_i and v_j are from different sets. Therefore, positive neighbors only exist in the same subset (i.e., either $\mathcal{V}_1$ or $\mathcal{V}_2$), while negative neighbors come from different subsets, which indicates that the signed graph $\mathcal{G}$ is structurally balanced by Definition 1. □

Note that homology and cohomology are computable topological invariants and various existing methods can be used to verify if the first homology or cohomology is vanishing (Edelsbrunner & Harer, 2010). Theorem 1 indicates that, if a simplicial complex $X_\mathcal{G}$ has a vanishing first cohomology $\mathcal{H}^1(X_\mathcal{G}; \mathbb{Z}_2) = 0$, the existence of the structural balance in $\mathcal{G}$ can be verified by only checking whether all 3-node circular subgraphs are positive. In addition, the developed characterization based on the vanishing cohomology in Theorem 1 unravels the fundamental relationship between the structural balance and the network structure from a global topological perspective. Since homology has an intuitive interpretation as "holes" in the constructed simplicial complex, the following corollary shows how Theorem 1 can be extended based on the first homology.

Corollary 1. *The signed graph $\mathcal{G}$ is structurally balanced if all 3-node circular subgraphs are positive and the first homology satisfies $\mathcal{H}_1(X_\mathcal{G}; \mathbb{Z}) = 0$, where $X_\mathcal{G}$ is the simplicial complex constructed from $\mathcal{G}$.*

The universal coefficient theorem for cohomology in Hatcher (2001) indicates that, if the first homology satisfies $\mathcal{H}_1(X_\mathcal{G}; \mathbb{Z}) = 0$, the first cohomology must have $\mathcal{H}^1(X_\mathcal{G}; \mathcal{A}) = 0$, where $\mathcal{A}$ is an abelian group. Therefore, Corollary 1 is a direct consequence of Theorem 1, where the abelian group $\mathcal{A}$ takes a particular form of $\mathbb{Z}_2$.

Remark 1. Compared to the condition of $\mathcal{H}^1(X_\mathcal{G}; \mathbb{Z}_2) = 0$ in Theorem 1, a stronger condition of $\mathcal{H}_1(X_\mathcal{G}; \mathbb{Z}) = 0$ is required in Corollary 1. Note that $\mathcal{H}_1(X_\mathcal{G}; \mathbb{Z}) = 0$ can be true for a variety of networks. For instance, there is a high probability that the first homology vanishes in large random graphs (Kahle, 2009).

Corollary 2. *A complete signed graph $\mathcal{G}$ is structurally balanced if all 3-node circular subgraphs are positive.*

It is well known that a complete graph always has vanishing homologies (Hatcher, 2001). Therefore, when considering a complete signed graph $\mathcal{G}$, the condition of $\mathcal{H}_1(X_\mathcal{G}; \mathbb{Z}) = 0$ in Corollary 1 can be further relaxed in Corollary 2. When $\mathcal{G}$ is complete, the verification of the structural balance boils down to checking whether all 3-node circular subgraphs in $\mathcal{G}$ are positive.

Theorem 2. *Consider a signed graph $\mathcal{G}$ modeled by a simplicial complex $X_\mathcal{G}$, where the first homology $\mathcal{H}_1(X_\mathcal{G}; \mathbb{Z})$ is nonzero. The signed graph $\mathcal{G}$ is structurally balanced if and only if all 3-node circular subgraphs are positive and the circular subgraphs corresponding to the nonzero $\mathcal{H}_1(X_\mathcal{G}; \mathbb{Z})$ are also positive.*

Proof. Since $\mathcal{H}_1(X_\mathcal{G}; \mathbb{Z})$ is nonzero, there must exist concatenated 1-simplices (e.g., a path in $\mathcal{G}$) forming one-dimensional holes in $X_\mathcal{G}$. Without loss of generality, only 1 one-dimensional hole is considered in the following analysis. For the case of multiple one-dimensional holes, the same analysis can be repeated for each hole.

Let $\mathcal{G}_\mathcal{H} = (\mathcal{V}_\mathcal{H}, \mathcal{E}_\mathcal{H}, \mathcal{W}_\mathcal{H})$ be the circular subgraph in $\mathcal{G}$ corresponding to the one-dimensional hole in $X_\mathcal{G}$. If $\mathcal{G}_\mathcal{H}$ is positive, $\mathcal{G}_\mathcal{H}$ is structurally balanced (Altafini, 2013), which indicates that $\mathcal{V}_\mathcal{H}$ can be divided into two sets $\mathcal{V}_{\mathcal{H}1}$ and $\mathcal{V}_{\mathcal{H}2}$ with $\mathcal{V}_{\mathcal{H}1} \cup \mathcal{V}_{\mathcal{H}2} = \mathcal{V}_\mathcal{H}$ and $\mathcal{V}_{\mathcal{H}1} \cap \mathcal{V}_{\mathcal{H}2} = \emptyset$ such that edges within each set are positive and edges connecting different sets are negative. Note that $\mathcal{G}_\mathcal{H}$ remains structurally balanced by Definition 1, if $\mathcal{G}_\mathcal{H}$ is augmented to a complete graph $\mathcal{G}'_\mathcal{H}$ by adding positive edges to nodes that are not connected in the same set, and negative edges between nodes from different sets. Since $\mathcal{G}'_\mathcal{H}$ is a complete graph, $\mathcal{G}'_\mathcal{H}$ is contractible and thus has the vanishing first homology, which indicates all circular subgraphs in $\mathcal{G}'_\mathcal{H}$ are positive. Together with the condition that all 3-node circular subgraphs are positive, the original graph $\mathcal{G}$ is also structurally balanced by Theorem 1.

To prove the necessary condition, note that a connected signed graph $\mathcal{G}$ is structurally balanced if and only if all circular subgraphs of $\mathcal{G}$ are positive, i.e., the product of edge weights on any circular subgraph is positive (Altafini, 2013). Consequently, all 3-node circular subgraphs and the circular subgraphs corresponding to the nonzero $\mathcal{H}_1(X_\mathcal{G}; \mathbb{Z})$ are all positive. □

Theorem 2 develops a necessary and sufficient condition to characterize the structural balance. Specifically, Theorem 2 relates the structure balance to the 3-node circular subgraphs, which provides insights into the key topological structures that result in the structural balance. If a graph does not have 3-node circular subgraphs, Theorem 2 is relaxed to only require that the circular subgraphs corresponding to the nonzero $\mathcal{H}_1(X_\mathcal{G}; \mathbb{Z})$ are all positive. Note that the developed characterizations are only applicable to undirected graphs, since Theorems 1 and 2 are developed based on a multiplicative abelian group $(\mathbb{Z}_2, \times)$, where only the product of edge weights matters in characterizing the structural balance. The direction of edges is not accounted for in the considered multiplicative abelian group. Ongoing research will consider other abelian groups taking into account the direction of edges if directed graphs are considered. Nevertheless, the revealed key topological structures can be leveraged in topology design (see Section 3.3 for an illustrative example).

Example 3. Fig. 3 is provided to illustrate the general ideas in the proof of Theorem 2. Consider a simplicial complex $X_\mathcal{G}$ consisting of six vertices (0-simplices), eight edges (1-simplices), and two 2-simplices (filled triangles) in Fig. 3(a). The vertices $\{1, 2, 3\}$ and $\{2, 4, 5\}$ form two positive 3-node circular subgraphs, while the vertices $\{2, 3, 6, 5\}$ form a one-dimensional hole in $X_\mathcal{G}$, indicating $\mathcal{H}_1(X_\mathcal{G}; \mathbb{Z}) \neq 0$. Fig. 3(b) shows the construction of a complete

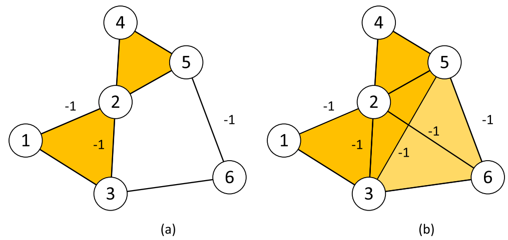

Fig. 3. The illustration of the proof of Theorem 2.

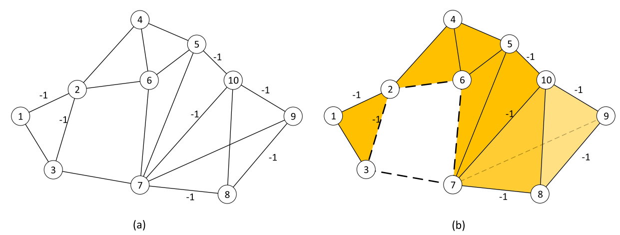

Fig. 4. (a) The structurally unbalanced signed graph $\mathcal{G}$. (b) The simplicial complex $X_{\mathcal{G}}$ constructed from $\mathcal{G}$, where the dashed lines indicate a one-dimensional hole.

subgraph over $\{2, 3, 6, 5\}$, which can be verified to be structurally balanced. Note that, in Fig. 3(b), its first homology $\mathcal{H}_1$ becomes zero due to the absence of the 1 dimensional hole, where Theorem 1 can be invoked to show that both Fig. 3(a) and (b) are structurally balanced.

3.3. Topology design

In this section, we will demonstrate the effectiveness of the developed topological characterizations of the structural balance and how the characterizations can be potentially extended to construct structurally balanced graphs via topology design.

Consider a signed graph $\mathcal{G}$ in Fig. 4(a), where negative edges are marked by -1. The signed graph $\mathcal{G}$ is initially structurally unbalanced. To demonstrate the developed topological characterizations of the structural balance in Section 3.2, $\mathcal{G}$ is represented by a simplicial complex $X_{\mathcal{G}}$ in Fig. 4(b), which consists of 10 0-simplices (nodes), 18 1-simplices (edges), 9 2-simplices (triangles), and 1 3-simplex (tetrahedron). It can be verified that all 2-simplices (i.e., 3-node circular subgraphs) are positive, while the vertices $\{3, 2, 6, 7\}$ form a one-dimensional hole (dashed lines), which indicates a non-vanishing first homology $\mathcal{H}_1(X_{\mathcal{G}}; \mathbb{Z}) \neq 0$. Since the one-dimensional hole formed by $\{3, 2, 6, 7\}$ is indeed a negative 4-node circular subgraph, the conditions in Theorem 2 are not satisfied, which is consistent with the fact that $\mathcal{G}$ is structurally unbalanced.

In $X_{\mathcal{G}}$, all 2-simplices are positive, and the only violation to Theorem 2 is the non-vanishing $\mathcal{H}_1$ formed by the vertices $\{3, 2, 6, 7\}$. If $\mathcal{G}$ is modified by removing the edge $\{3, 7\}$, the vertices $\{3, 2, 6, 7\}$ no longer form a one-dimensional hole, and thus $\mathcal{H}_1(X_{\mathcal{G}}; \mathbb{Z}) = 0$, which indicates that the modified $\mathcal{G}$ becomes structurally balanced by Corollary 1. Note that the removal of $\{3, 7\}$ is not the only way to construct a structurally balanced graph from $\mathcal{G}$. An alternative is to switch the edge weight of $\{3, 7\}$ from $+1$ to -1, resulting in a positive circular subgraph of $\{3, 2, 6, 7\}$. Theorem 2 can then be invoked to indicate that the modified $\mathcal{G}$ with a negative weight on $\{3, 7\}$ is also structurally balanced.

Remark 2. The developed algebraic topological characterizations can not only verify the structural balance, but also provide insights on how to tweak the network topology to yield structural balance. What makes the topological characterizations powerful is their capability to identify the key structures (i.e., one-dimensional holes) or key components (i.e., certain edges) in the graph, such that a minor modification on these key structures or components can result in a significant change of network topology structures, e.g., a change from structural unbalance to structural balance. Such insights are generally not obtainable from standard graphical methods and conventional analysis tools. The key enablers in our approach are the use of the novel simplicial-complex-based modeling approach capturing the global topological structure of the signed graph, and tools such as homology and cohomology to extract topological properties crucial to the structural balance.

4. Discussion and conclusion

Algebraic topological characterizations of the structural balance in signed graphs are developed in this work. Leveraging tools from algebraic topology, simplicial complexes are used to model signed graphs, upon which simplicial homology and cohomology based characterizations are developed to capture the topological properties of the structural balance. The effectiveness of the developed topological characterizations is demonstrated via examples. Additional research will continue along this direction and further explore how the developed topological characterizations can be utilized in topology design for desired network performance. Specifically, based on (Aref & Wilson, 2017), additional research will investigate the potential extension of the developed cycle based topological characterizations in measuring partial balance in signed graphs. Future research will also consider extending the work of Yaghmaie, Su, Lewis, and Xie (2017) and investigate the topological characterizations of generalized structural balance of graphs with complex edge weights.

Acknowledgment

This work was supported by the Air Force Research Lab under Grant FA9453-19-1-0077.

References

Alemzadeh, S., de Badyn, M. H., & Mesbahi, M. (2017). Controllability and stabilizability analysis of signed consensus networks. In *IEEE conf. control technol. appl.* (pp. 55–60). IEEE.

Altafini, C. (2013). Consensus problems on networks with antagonistic interactions. *IEEE Transactions on Automatic Control*, *58*(4), 935–946.

Antal, T., Krapivsky, P. L., & Redner, S. (2005). Dynamics of social balance on networks. *Physical Review E*, *72*(3), 036121.

Aref, S., & Wilson, M. C. (2017). Measuring partial balance in signed networks. *Journal of Complex Networks*, *6*(4), 566–595.

de Badyn, M. H., Alemzadeh, S., & Mesbahi, M. (2017). Controllability and data-driven identification of bipartite consensus on nonlinear signed networks. arXiv preprint arXiv:1709.06679.

Chintakunta, H., & Krim, H. (2014). Distributed localization of coverage holes using topological persistence. *IEEE Transactions on Signal Processing*, *62*(10), 2531–2541.

Choi, H.-L., & How, J. P. (2011). Efficient targeting of sensor networks for large-scale systems. *IEEE Transactions on Control Systems and Technology*, *19*(6), 1569–1577.

Crossley, N. A., Mechelli, A., Vértes, P. E., Winton-Brown, T. T., Patel, A. X., Ginestet, C. E., McGuire, P., & Bullmore, E. T. (2013). Cognitive relevance of the community structure of the human brain functional coactivation network. *Proceedings of the National Academy of Sciences of the United States of America*, *110*(28), 11583–11588.

De Silva, V., & Ghrist, R. (2006). Coordinate-free coverage in sensor networks with controlled boundaries via homology. *International Journal of Robotics Research*, *25*(12), 1205–1222.

Durbin, J. R. (2008). *Modern algebra: An introduction*. John Wiley & Sons.

Edelsbrunner, H., & Harer, J. (2010). *Computational topology: an introduction*. American Mathematical Soc..

Fang, X., Misra, S., Xue, G., & Yang, D. (2012). Smart grid - The new and improved power grid: A survey. *IEEE Communications Surveys and Tutorials*, *14*(4), 944–980.
Girvan, M., & Newman, M. E. (2002). Community structure in social and biological networks. *Proceedings of the National Academy of Sciences of the United States of America*, *99*(12), 7821–7826.
Harary, F. (1960). A matrix criterion for structural balance. *Naval Research Logistics*, *7*(2), 195–199.
Harary, F., & Kabell, J. A. (1980). *A simple algorithm to detect balance in signed graphs*. Elsevier.
Harary, F., et al. (1953). On the notion of balance of a signed graph. *The Michigan Mathematical Journal*, *2*(2), 143–146.
Hatcher, A. (2001). *Algebraic topology*. New York: Cambridge University Press.
Jackson, M. O. (2010). *Social and economic networks*. Princeton University Press.
Jiang, Y., Zhang, H., & Chen, J. (2017). Sign-consensus of linear multi-agent systems over signed directed graphs. *IEEE Transactions on Industrial Electronics*, *64*(6), 5075–5083.
Kahle, M. (2009). Topology of random clique complexes. *Discrete Mathematics*, *309*(6), 1658–1671.
Kan, Z., Dani, A., Shea, J. M., & Dixon, W. E. (2012). Network connectivity preserving formation stabilization and obstacle avoidance via a decentralized controller. *IEEE Transactions on Automatic Control*, *57*(7), 1827–1832.
Kunegis, J. (2014). Applications of structural balance in signed social networks. arXiv preprint arXiv:1402.6865.
Liu, J., Chen, X., & Başar, T. (2016). Stability of the continuous-time Altafini model. In *Am. control conf.* (pp. 1930–1935). IEEE.
Marvel, S. A., Kleinberg, J., Kleinberg, R. D., & Strogatz, S. H. (2011). Continuous-time model of structural balance. *Proceedings of the National Academy of Sciences*, *108*(5), 1771–1776.
Meng, D., Meng, Z., & Hong, Y. (2018). Uniform convergence for signed networks under directed switching topologies. *Automatica*, *90*, 8–15.
Olfati-Saber, R., Fax, J. A., & Murray, R. M. (2004). Consensus problems in networks of agents with switching topology and time-delays. *IEEE Transactions on Automatic Control*, *49*(9), 1520–1533.
Pan, L., Shao, H., & Mesbahi, M. (2016). Verification and prediction of structural balance: A data-driven perspective. In *Proc. am. control conf.* (pp. 2858–2863). IEEE.
Proskurnikov, A. V., Matveev, A. S., & Cao, M. (2016). Opinion dynamics in social networks with hostile camps: Consensus vs. polarization. *IEEE Transactions on Automatic Control*, *61*(6), 1524–1536.
Ren, W., Beard, R. W., & Atkins, E. M. (2007). Information consensus in multi-vehicle cooperative control. *IEEE Control Systems Magazine*, *27*, 71–82.
Sun, C., Hu, G., & Xie, L. (2017). Controllability of multi-agent networks with antagonistic interactions. *IEEE Transactions on Automatic Control*, *62*(10), 5457–5462.
Tahbaz-Salehi, A., & Jadbabaie, A. (2010). Distributed coverage verification in sensor networks without location information. *IEEE Transactions on Automatic Control*, *55*(8), 1837–1849.
Tanner, H. G., Jadbabaie, A., & Pappas, G. J. (2007). Flocking in fixed and switching networks. *IEEE Transactions on Automatic Control*, *52*(5), 863–868.
Wu, Y., Zhao, Y., & Hu, J. (2017). Bipartite consensus control of high-order multi-agent systems with unknown disturbances. *IEEE Transactions on Systems, Man, and Cybernetics*.
Yaghmaie, F. A., Su, R., Lewis, F. L., & Xie, L. (2017). Multiparty consensus of linear heterogeneous multiagent systems. *IEEE Transactions on Automatic Control*, *62*(11), 5578–5589.
Yaïche, H., Mazumdar, R. R., & Rosenberg, C. (2000). A game theoretic framework for bandwidth allocation and pricing in broadband networks. *IEEE/ACM Transactions on Networking*, *8*(5), 667–678.
Zhang, H., & Chen, J. (2017). Bipartite consensus of multi-agent systems over signed graphs: State feedback and output feedback control approaches. *International Journal of Robust and Nonlinear Control*, *27*(1), 3–14.

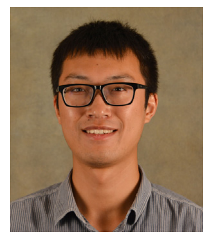

Baike She received the B.S. degree in Electrical Engineering from the Sichuan University in 2013 and the M.S. degree in Control Engineering from the University of Science and Technology of China in Control Engineering in 2016. He is currently pursuing the doctoral degree in mechanical engineering at the University of Iowa under the supervision of Dr. Zhen Kan. His current research interests include control of multi-agent systems, complex networks, and algebraic topology.

Zhen Kan is a professor in the Department of Automation at University of Science and Technology of China. He received his Ph.D. degree in 2011 from the Department of Mechanical and Aerospace Engineering at the University of Florida. He was a Postdoctoral Research Fellow with the Air Force Research Laboratory (AFRL) at Eglin AFB and University of Florida REEF from 2012 to 2016, and was an Assistant Professor in the Department of Mechanical Engineering at the University of Iowa. His current research interests include networked robotic systems, Lyapunov-based nonlinear control, graph theory, complex networks, and human-assisted estimation, planning, and decision making. He currently serves as an Associate Editor on Conference Editorial Board in IEEE Control Systems Society and technical committee for several internationally recognized scientific and engineering conferences.